

Effect of Cathode Position on Hall-Effect Thruster Performance and Cathode Coupling Voltage

Jason D. Sommerville* and Lyon B. King

Michigan Technological University, Houghton, Michigan 49931, USA

Hall-effect thruster performance as a function of cathode position is explored through a series of experiments in which performance is monitored while the cathode is translated via a 2-axis motion table. Significant changes in thrust, efficiency, and cathode coupling voltage are observed. Efficiency changes as great as 12% are measured. Cathode coupling voltages typically move closer to ground as the cathode is moved away from the thruster in the radial direction and as it is moved forward of the exit plane. Corresponding improvements in performance are measured. However, the improvements in performance are greater than can be explained by the change in cathode coupling voltage alone. The performance data is compared to the modeled magnetic field structure external to the thruster. This comparison suggests that better performance is achieved when the cathode is placed such that magnetic field lines guide the cathode electrons closer to the discharge channel.

Nomenclature

a	Acceleration losses
e	Electronic charge
f_i	Propellant ionization fraction
I	Anode supply current
\dot{m}	Anode mass flow
m_i	Mass of a xenon ion
n_q	Density of xenon neutral or ion with charge state q
\bar{q}	Average xenon species charge number
T	Thrust
t	Time
T_f	Final measurement of thrust with thruster off. (Thrust stand drift.)
$\langle v \rangle$	Magnitude of the average exit velocity of the HET beam
V	Discharge voltage. Potential difference between the anode and the cathode.
V_{acc}	Maximum ion beam acceleration potential
V_{cg}	Cathode coupling voltage (< 0)

Symbols

η	Thruster efficiency
η_{cg}	Efficiency due to cathode coupling
η_{other}	Other HET efficiency terms

I. Introduction

Hall-effect thrusters (HETs) are a class of electric propulsion devices that use electric and magnetic fields to create a plasma and expel the ions at high velocity in order to generate thrust.¹ A critical component of the HET is the cathode. The cathode in an HET is a plasma source which provides free electrons which serve two purposes. The first purpose is beam neutralization—sufficient electrons are expelled via the cathode to balance the charge emitted by the ion beam. The second purpose is to provide the “seed” electrons which initialize and sustain the plasma discharge near the exit plane of the HET.

*ME-EM Dept., 815 R.L. Smith Bldg., 1400 Townsend Dr.

The cathode coupling voltage (V_{cg}) is one of the most important parameters that quantifies cathode coupling behavior. In the laboratory, this parameter is the potential difference between the cathode and ground, i.e. the tank walls, and is always a negative value. In space, the concept remains valid, the ground of the tank walls being replaced with the plasma potential infinitely far from the spacecraft. Since the anode is usually referenced to the cathode, the maximum potential through which the beam ions fall is $V_{acc} = V + V_{cg}$ and the maximum energy that can be imparted to a beam ion is qeV_{acc} . To illustrate this, Figure 1 schematically compares a low coupling voltage, V_{cg1} , to a high coupling voltage, V_{cg2} . Note that in both cases the anode voltage, V , is the same; the same amount of energy must be provided by the power supply. Therefore, lower (further from ground) coupling voltages give rise to greater losses in the thruster efficiency, as less acceleration is provided for the same energy cost.

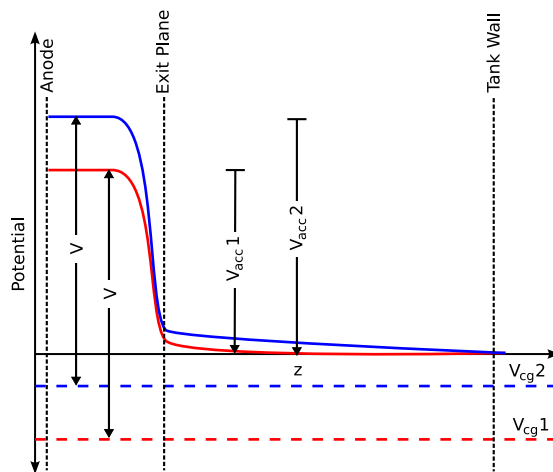


Figure 1: The available acceleration voltages, V_{acc} , for low and high cathode coupling voltages, V_{cg1} , and V_{cg2} .

The coupling voltage provides a measure of how easily electrons are transported from the cathode to the anode. Visualizing the electric circuit between the cathode and the anode as a simple ohmic circuit, lower voltages (that is, greater in magnitude) imply that there is a larger resistance between the cathode and the anode, and therefore more energy is lost in the process of providing electrons to the discharge chamber of the cathode.

The process by which the free electrons in the plume of the cathode are coupled to the anode of an HET and how this process affects cathode coupling voltage and thruster performance is not well understood. A few researchers have studied the effects of cathode type² and mass flow rate^{2,3} on HET performance. Albaréde, et al. compared three types of thermionic orificed cathodes and found only small differences in behavior.² Both Albaréde, et al. and Tilley, et al. observed increases in cathode coupling voltage with increasing flow rate, and Albaréde, et al. also noticed non-monotonic changes in anode current fluctuation frequency with changes in cathode mass flow.² It has been repeatedly noted that cathode placement has an effect on thruster performance.⁴⁻⁶ Hofer, et al. noticed significant performance improvements by placing the cathode in the center of the HET rather than outside,⁴ and Beal, Galimore and Hargus have inferred from probe measurements that cathode placement and number in an HET cluster will affect performance.⁶ However, to the best of our knowledge, only the study by Tilley, et al. specifically addresses the effect of cathode position on HET performance and is available in the literature.³ In that study, the authors note an increase in cathode coupling voltage as the cathode is moved forward of the exit plane.

There has been recent interest in the field of electric propulsion in scaling thrusters to lower voltages in order to achieve high thrust-to-power ratios.⁷⁻¹⁰ As V is decreased, the same coupling voltage represents a greater efficiency hit as it becomes a larger portion of the total available voltage. Therefore any optimization in the cathode coupling voltage at low thruster voltage may represent a significant gain in thruster efficiency.

In this work we study the performance of an HET as a function of cathode position, discharge voltage and magnet current. We then compare the performance data with the magnetic environment in which the cathode operates, as determined by a model, and propose two mechanisms whereby cathode placement affects HET-cathode coupling and HET performance.

II. Experiment

As a first step in gaining a greater understanding of cathode to HET coupling, we have undertaken a series of experiments studying the performance of an HET as a function of radial and axial cathode position. Given the interest in low power HETs, we have operated at voltages from 300 down to 150 V at optimal magnet current. For select operating voltages we have also varied the magnet current to sub- and super-optimal values. All experiments were performed with a BPT-2000 HET and a laboratory cathode at Michigan Tech's Ion Space Propulsion Laboratory.

A. Equipment

1. Vacuum Facility

All experiments were run in the Xenon Vacuum Facility at Michigan Tech's Ion Space Propulsion Laboratory. The facility is a 4-m-long chamber 2 m in diameter. It is evacuated by two 48-inch cryogenic pumps capable of 60,000 L/s each. The base pressure during these experiments was 1.3×10^{-5} Torr and operating pressures were 3.8×10^{-5} Torr as measured by an ion gauge corrected for xenon and located in the back third of the chamber.

2. Hall Thruster

The HET used in this experiment was an Aerojet BPT-2000, 2 kW class thruster.¹¹ The thruster has an outer diameter of ~100 mm and a channel width of ~10 mm. It operates at a nominal voltage of 300 V and a mass flow of 5 mg/s xenon. At these conditions its specific impulse is ~1700 s with ~50% efficiency.

3. Cathode

The cathode used in these experiments was a laboratory cathode similar to the MIREA cathode used by Albadère.² It is shown schematically in Figure 2. The cathode consists of a 1-inch-diameter titanium cylinder approximately 100 mm long. A 2-mm orifice was drilled in one face. Pressed against this hole is a molybdenum pellet holder which holds a lanthanum-hexaboride (LaB_6) emitter. Xenon is introduced into the cathode via a feed tube attached to the side of the cylinder. Filling the length of the cathode from the pellet holder to the base is a tungsten heater coil which heats the emitter to its operating temperature. Radiation insulation loosely wraps the heater and pellet holder to maximize emitter heating. A keeper electrode is positioned approximately 3 mm outside of the orifice and is used to ignite and maintain the cathode discharge.

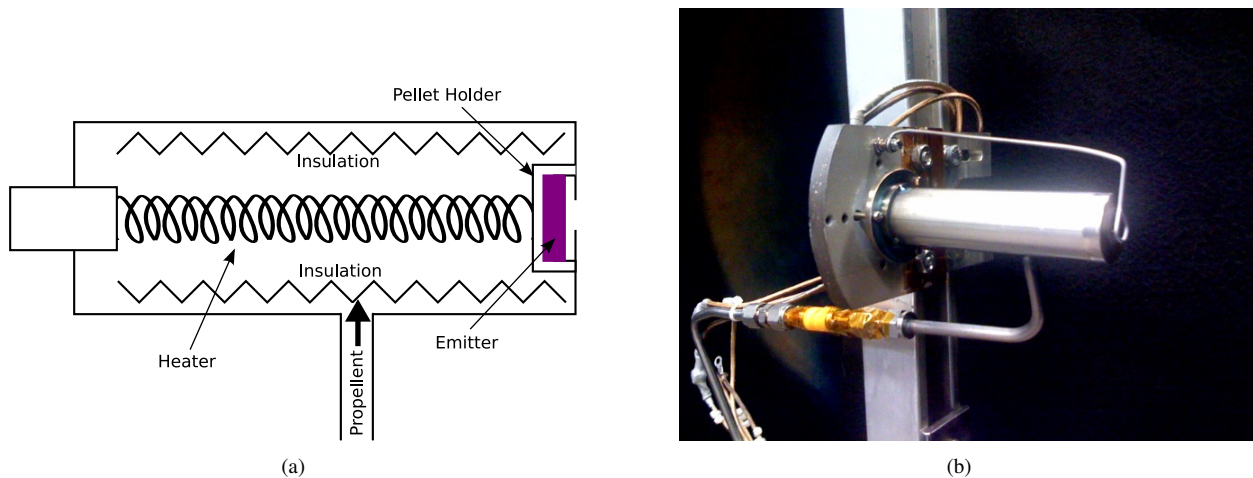


Figure 2: (a) Schematic representation of the laboratory cathode. (b) Photograph.

4. Mass Flow Controllers

Flow of xenon to the thruster and the cathode was controlled by MKS Type 1479a mass flow controllers. Their accuracy has been tested by monitoring the rise in pressure of a small calibration tank of known volume while flowing gas into the tank. The mass flow controllers are accurate to 5% of the full scale reading: 200 SCCM (19.5 mg/s xenon) for the anode controller, and 20 SCCM (1.95 mg/s xenon) for the cathode controller.

5. Thrust Stand

The thrust stand is a NASA-Glenn style, null displacement, inverted pendulum thrust stand, with automatic leveling. The displacement nulling is provided by a solenoid driven by a closed-loop digital controller which reads the displacement on an LVDT. The level is read by an electrolytic inclinometer, and controlled by a microstepping motor connected to an 80-threads-per-inch screw. The thrust is directly proportional to the current provided to the solenoid. Calibration is provided by a linear fit to a set of known weights applied to the thruster across a pulley and controlled via a stepper motor.

The closed loop controls on this thrust stand were recently implemented, and these experiments were the first to take advantage of them. During the experiment, it became clear that the level control was less than optimal. The stepper motor introduced excessive vibrations into the system which were recorded as vibrations in the thrust. Additionally, the screw attached to the stepper motor did not always rotate the same distance as the stepper motor. Rather, the screw would torque, and then eventually release several updates worth of rotation in a single, jarring motion. Averaging the thrust over a minute or two served to partially mitigate these problems.

Despite the continuous leveling, we recorded drifts in thrust measurements over time under some operating conditions. We confirmed these drifts as measurement errors by noting the thrust measurement after thruster shutdown. If no drift occurred, the thrust stand would read approximately zero thrust. In some cases, however, the thrust stand drifted as much as 5 mN over 120 minutes. The source of the drift is not entirely clear. Investigations concurrent with the present experiments suggest that thermal changes in the thruster mount cause small changes in the position of the thruster with respect to the thrust stand, which in turn effects a change in the recorded thrust. Modifications to the setup were made over the course of the experiment, specifically between Tests 5 and 6 (see Section B), which reduced, but did not eliminate the drifts.

To attempt to correct the drifts in thrust stand level, we have assumed a linear drift over the period from thruster turn on to thruster turn off. The slope of the drift is assumed to be T_f/t and the final thrust is given by

$$T(t) = T_{meas} - T_f/t. \quad (1)$$

The efficiency is calculated from the thrust according to

$$\eta = \frac{T^2}{2\dot{m}IV}. \quad (2)$$

Note that \dot{m} does not include cathode mass flow, and likewise, I and V measure only the current through and voltage to the anode.

Given the drifts in the thrust stand compounded with the error in the linear fit, the error in the thrust measurement is estimated at 5%. Propagating the errors of the thrust measurement and the mass flow rate through the efficiency equation, we estimate the error on the efficiency measurements at 9% of the stated values.

B. Cathode Position Experiment

To quantify the effect of cathode position on thruster performance, we ran the BPT-2000 mounted on the thrust stand, while moving the cathode through radial and axial sweeps. Data acquisition hardware and software was used to record thrust, anode current, mass flow, and cathode coupling voltage. Thruster efficiency was calculated by the software according to Equation 2.

For these tests the cathode was mounted on a two-axis motion table as shown in Figure 3. This setup enabled us to place the cathode at radial displacements of $0 \leq r \leq 250$ mm where 0 is as close to the thruster as the cathode can be positioned without contacting it (see close-up in Figure 3). At radial displacements greater than or equal to 50 mm the cathode could be positioned at axial displacements of -295 mm $\leq z \leq 900$ mm where at $z = 0$ the cathode face is even with the thruster face.

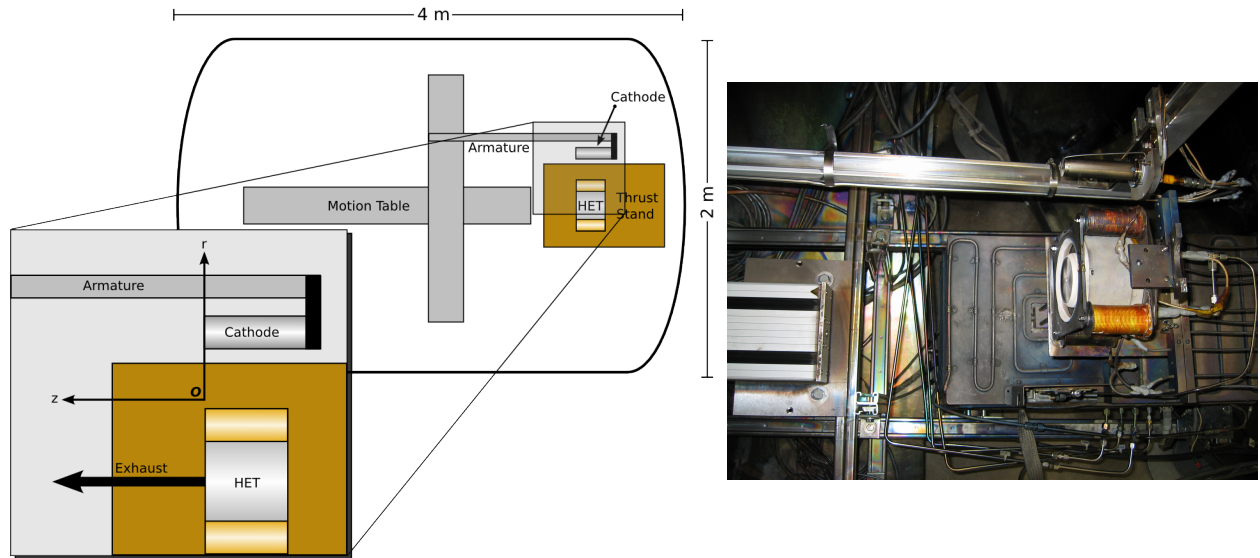


Figure 3: Experimental setup

Table 1: Cathode Position Tests

Test	V (V)	\dot{m} (mg/s)	I_{mag} (A)	Optimization	r	z
Test 1a	300	5.0	4.20	Optimal	$0 \leq r \leq 200$ mm	0 mm
Test 1b	300	5.0	3.15	Suboptimal	$0 \leq r \leq 200$ mm	0 mm
Test 1c	300	5.0	5.25	Superoptimal	$0 \leq r \leq 200$ mm	0 mm
Test 2a	250	4.0	2.5	Optimal	$0 \leq r \leq 200$ mm	0 mm
Test 2b	250	4.0	2.1	Suboptimal	$0 \leq r \leq 200$ mm	0 mm
Test 2c	250	4.0	3.15	Superoptimal	$0 \leq r \leq 200$ mm	0 mm
Test 3	200	4.0	2.1	Optimal	$0 \leq r \leq 200$ mm	0 mm
Test 4	150	4.0	0.6	Optimal	$0 \leq r \leq 200$ mm	0 mm
Test 5	250	4.0	2.5	Optimal	50 mm	$-150 \text{ mm} \leq z \leq 900$ mm
Test 6	250	4.0	2.5	Optimal	38 mm	$0 \text{ mm} \leq z \leq 400$ mm
Test 7	250	4.0	2.5	Optimal	78 mm	$-100 \text{ mm} \leq z \leq 500$ mm
Test 8	250	4.0	2.5	Optimal	157 mm	$-100 \text{ mm} \leq z \leq 700$ mm

Several radial and axial sweeps were performed at varying thruster operating conditions. Sweeps were typically conducted from $0 \leq r \leq 200$ mm in 10 mm increments. Table 1 shows the complete list of operating conditions. All conditions were performed with cathode mass flow rates of ~ 1 mg/s.

During each test the thruster was allowed to run at the operating point for at least 30 minutes prior to recording data to allow the thruster, cathode, and thrust stand to reach thermal equilibrium. After this period, the thruster was turned off, and thrust stand calibration performed. The calibration procedure typically required three minutes. Then, the thruster was run for two to three minutes at each of the cathode positions and the thrust data averaged over this period. The positions were selected in random order to avoid correlations between any temporal changes in thruster or thrust stand performance with changes due to cathode position. After all positions were measured, the thruster was turned off and any offset from 0 thrust measured by the thrust stand recorded (see Section 5).

In all cases, the thruster was first operated at its most efficient magnetic field, as determined by adjusting the magnetic current while monitoring the efficiency calculated in real time by the thrust stand software. This optimization was performed with the cathode at the origin. We later discovered that in nearly all cases this was the least efficient cathode position, and future tests will be optimized with the cathode in a better position. For consistency, the procedure was continued throughout all of the data presented here.

In Test 1 and Test 2, the 300 V and 250 V cases, the magnet current was adjusted above and below the optimal values. For the Test 1, values 25% above and below the optimal were chosen. For the Test 2, whose optimal magnet current was 2.5 A, values of 3.15 A and 2.1 A were chosen for the super- and sub-optimal currents because they matched magnet currents used in Test 1 and Test 3 respectively. Future tests are planned which will extend the procedure of magnet current adjustment to all cases.

Between Tests 5 and 6 the thruster was repositioned lower, closer to the thrust stand, to reduce thermal drifts in the thrust measurements. However, the cathode could no longer be positioned on the exact azimuthal position as in the previous tests. The displacements listed in Table 1 have been corrected to account for this.

III. Results

Figures 4 and 5 plot thrust, efficiency, anode current, and cathode coupling voltage as a function of cathode radial position for each of the radial tests. In all cases, when the cathode was near the thruster, particularly at $r = 0$, significant heat was exchanged between the cathode and the anode. This was evidenced by an increase in voltage in the current-limited supplies for the cathode heater and the magnet coils. This heat exchange made it difficult to achieve thermal equilibrium and the error on these data points is therefore significantly higher than on those where the cathode is positioned further from the thruster.

Test 1 is at the nominal operating point for the thruster. For all magnet currents, the cathode coupling voltage trends upwards as the cathode is moved away from the thruster, changing by approximately 10 V, or 3% of the discharge voltage. The anode current holds steady and the thrust increases, resulting in an efficiency increase of approximately 3% to 5%.

During Test 1c it was necessary to restart the thruster. The numbered points in Figure 4(c) show the order in which the points were taken, and the asterisk denotes the first point after the restart. We noted that the cathode coupling voltages did not return to exactly the same position after the restart.

Test 2, run at a discharge voltage of 250 V, shows the most interesting behavior. All magnetic field conditions exhibited a peak in cathode coupling voltage between 40 and 60 mm, followed by a trough between 80 and 100 mm, and then a gradual rise as the cathode was moved out to 200 mm. Again the discharge current held constant, while the thrust and efficiency tracked the changes in cathode coupling voltage.

Test 3, run at a discharge voltage of 200 V, also exhibits anomalies due to thruster restarts. Again, the plot shows the order in which the data were taken, with asterisks denoting the first point after a thruster restart. Note that there is a significant jump in cathode coupling voltage after the restart between points five and six. In particular, the cathode coupling voltage dropped by approximately 2 V between points thirteen and five. We believe that some of this drop is attributed to the change in conditions between thruster restarts. However, the magnitude of the change in cathode coupling voltages across the range of cathode positions is much smaller than in either Test 1 or Test 2.

Test 4, at a discharge voltage of 150 V, shows drastically different behavior than the previous tests. Here the cathode coupling voltage significantly decreases with increasing radial distance. The thrust and efficiency also decrease, somewhat in step with the cathode coupling voltage. Note also that the discharge current, in contrast to the other cases, changes drastically with cathode position.

Test 5 was performed at the optimal magnet current of 2.5 A and a discharge voltage of 250 V. Here, the cathode was placed 50 mm away from the thruster, radially. As the cathode was moved behind the thruster poor performance

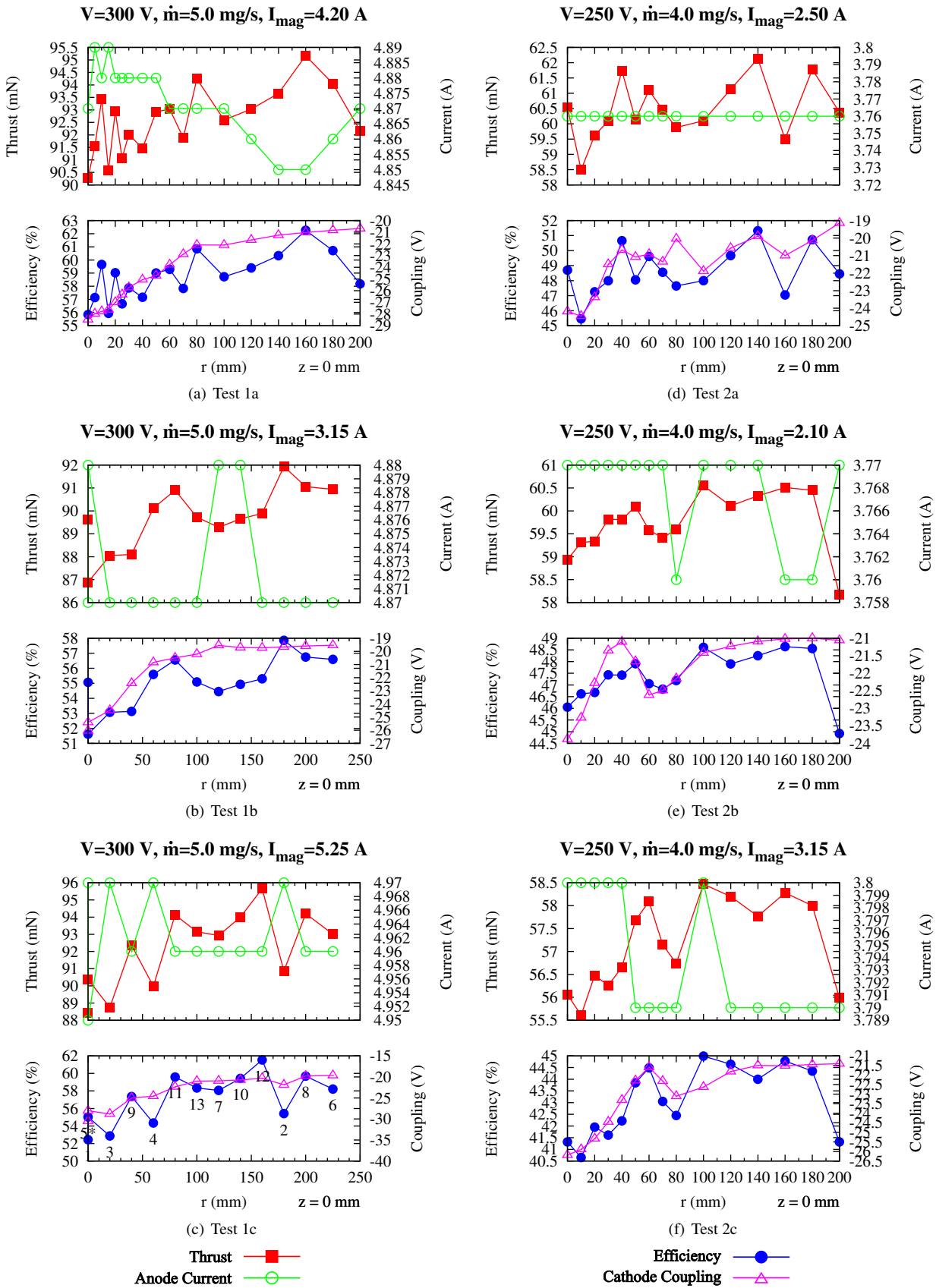


Figure 4: Results of the cathode position test

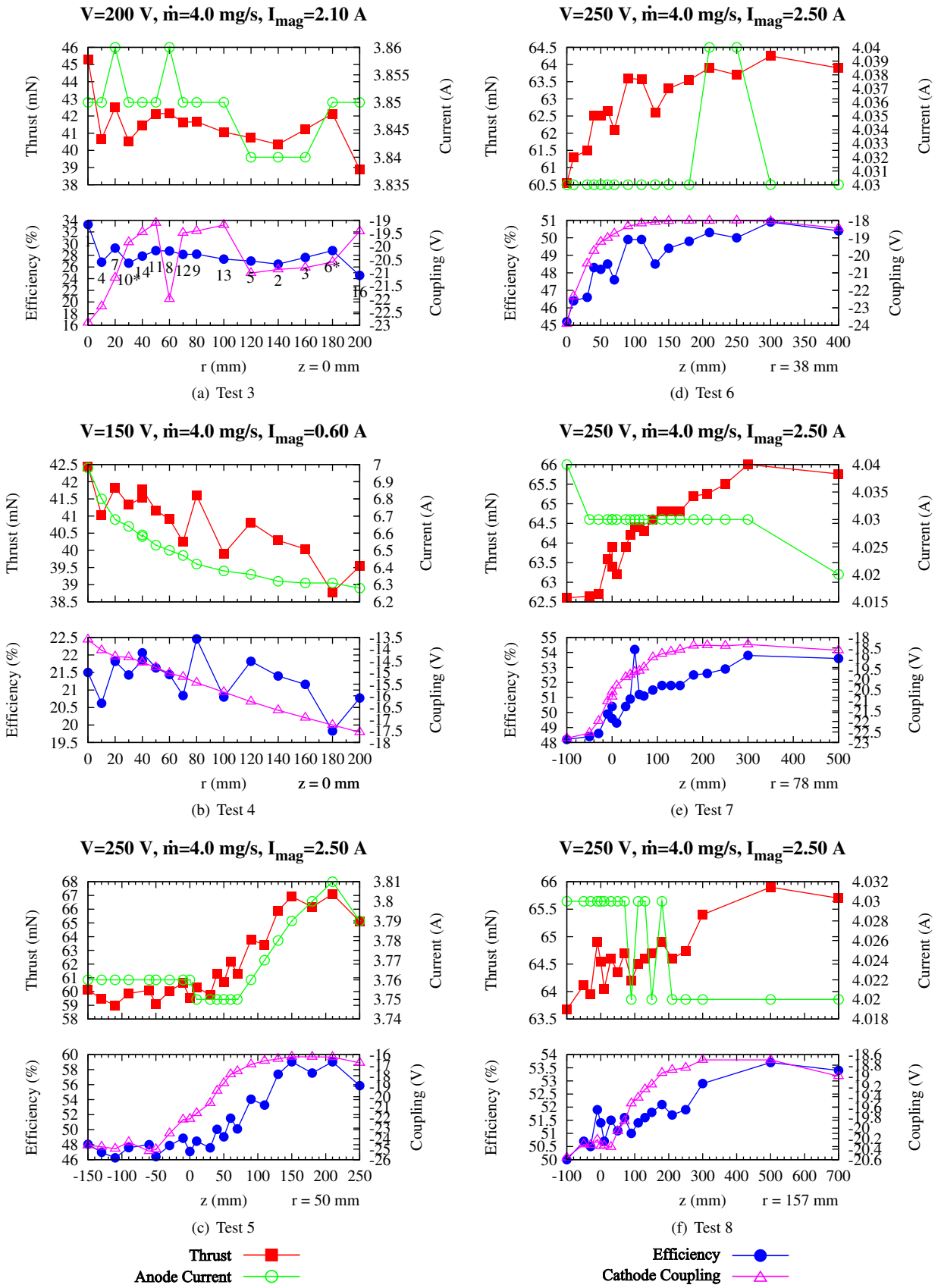


Figure 5: Results of the cathode position test (continued)

is recorded, along with low cathode coupling voltages. As the cathode was brought downstream of the thruster the performance of the thruster and cathode coupling voltage improved significantly, reaching a peak at 175 mm downstream of the exit plane. The anode current is seen to vary slightly, but consistently, with the other measurements. This change in current is small in comparison to Test 4, but certainly much more pronounced than the remainder of the radial sweeps.

Tests 6–8 were taken at the same operating conditions as Test 5, that is, optimal magnet current of 2.5 A at a discharge voltage of 250 V. However, these data were taken on a different day, following small modifications to the setup which were made in a partially successful attempt to further alleviate thermal drifts in the thrust stand. These data show good agreement in trends with the data taken in Test 5, particularly comparing Test 6 and Test 5 which were taken at nearby radial positions. The most notable difference between Test 5 and 6 is that the current is about 5% higher in Test 6, and does not change appreciably in Test 6 as it does in Test 5. The higher anode currents cause lower overall efficiencies in Test 6 as compared to Test 5. The reason for the change in current is not clear. One possibility is that the cathode is coupling to grounded surfaces differently due to the change in setup. None-the-less, the fact that the overall trends remain suggest that fundamental changes in cathode-HET coupling are occurring as the cathode position is changed.

Comparing Tests 6, 7, and 8 one consistently notes increasing cathode coupling voltages with increasing z , up to a maximal point. The maximum increases with increasing r , occurring at ~ 150 mm for $r = 38$ mm, ~ 200 mm for $r = 78$ mm, and ~ 300 mm for $r = 157$ mm. The thrust and efficiencies, again, loosely follow this trend, perhaps lagging behind a little as the coupling voltages begin to fall off.

IV. Magnetic Field Model

A. Model

Because electrons typically follow magnetic field lines, any substantial understanding of cathode coupling in HETs must take magnetic field structure into account. Therefore, we have modelled a simplified version of the BPT-2000 using a finite element magnetostatic field solver (Comsol Femlab) to determine the magnetic field produced at the various operating conditions.

The thruster is not radially symmetric, and thus, a 3-D model was required. However, the thruster does exhibit 8-fold symmetry; therefore, only one eighth of the thruster was modelled. The model is shown in Figure 6. The model and the surrounding vacuum was discretized meshed with approximately 50,000 tetrahedra and the field solved. A cross section of the field along the x -axis, the plane in which the cathode sits, was extracted. Using a hand-held gauss probe, the actual field strength of the thruster was measured at four locations outside the thruster and in this cross section. This was done with the magnet current set to 4.2 A. The model was found to match these values to within the 15% estimated accuracy of the measurements.

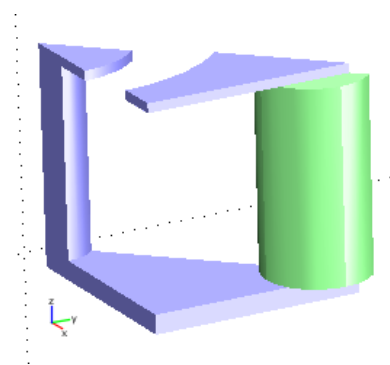


Figure 6: Model of the simplified HET magnetic circuit.

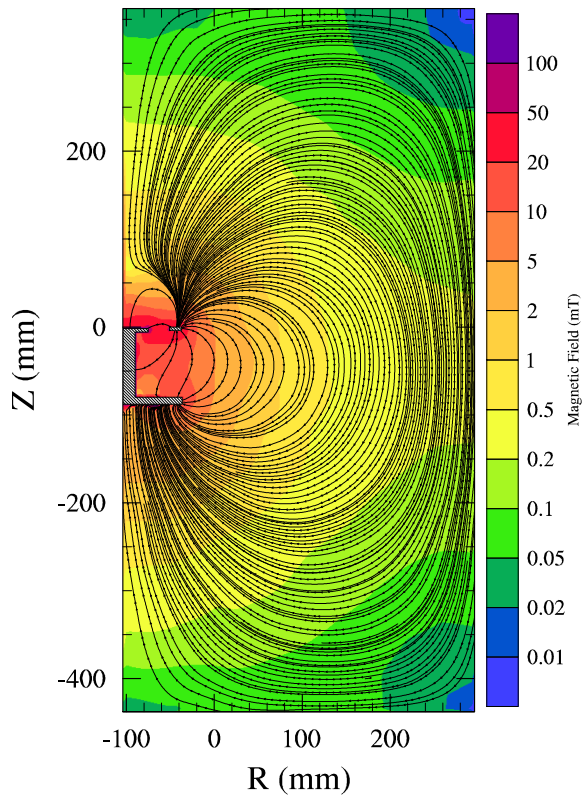
B. Model Results

The magnetic field model results are shown in Figure 7 for each of the optimal magnet current values. The first significant observation is that no field line will carry an electron into the discharge channel, as they all end at the thruster face, or the side of the face. Furthermore, the field lines clearly show that the electrons created near the thruster, particularly at $z = 0$ will be guided toward the outside edge of the front plate. It is not until $r > \sim 50$ mm that the lines curve significantly over to the front face of the plate. Finally, note that as the cathode is moved increasingly in r or in z the field lines bring the electrons closer to the discharge channel.

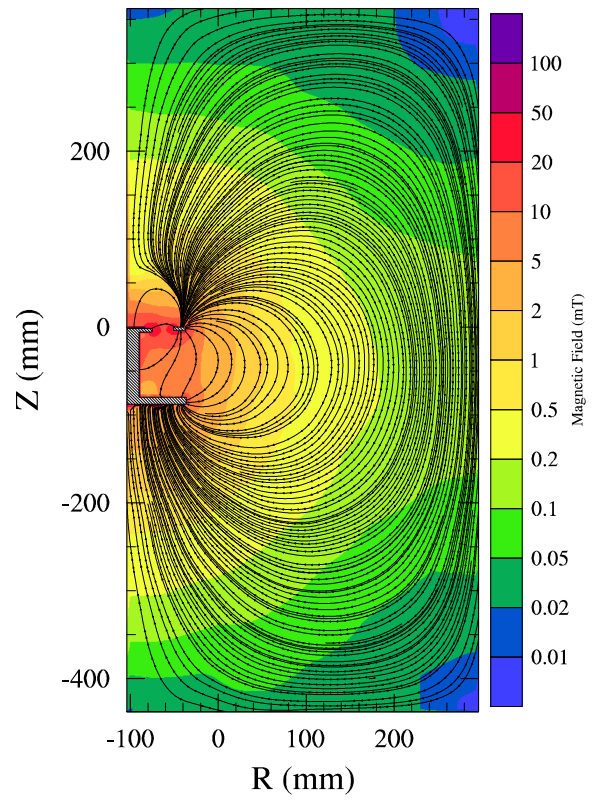
V. Discussion

A. Theoretical Effect of Cathode Coupling Voltage on Performance

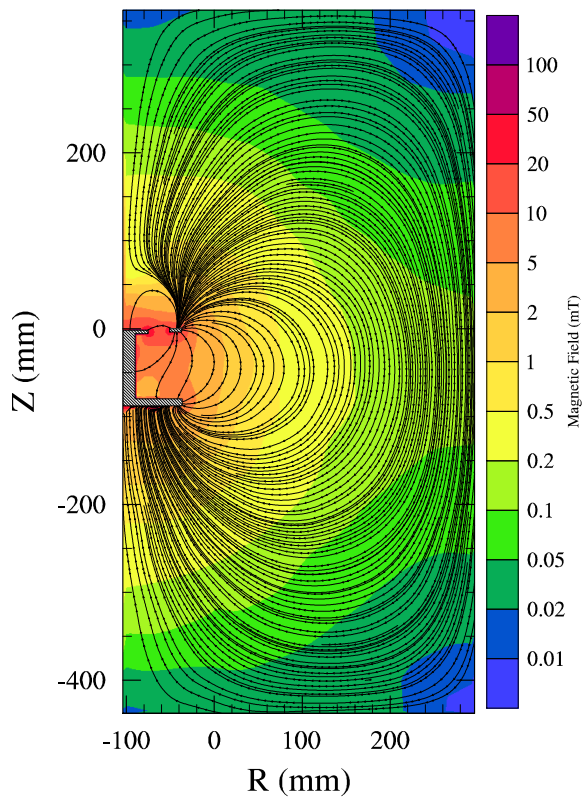
The cathode coupling voltage plays an important role in determining the overall performance of the thruster. As previously mentioned, cathode couple voltage provides a measure of how easily cathode electrons are transported



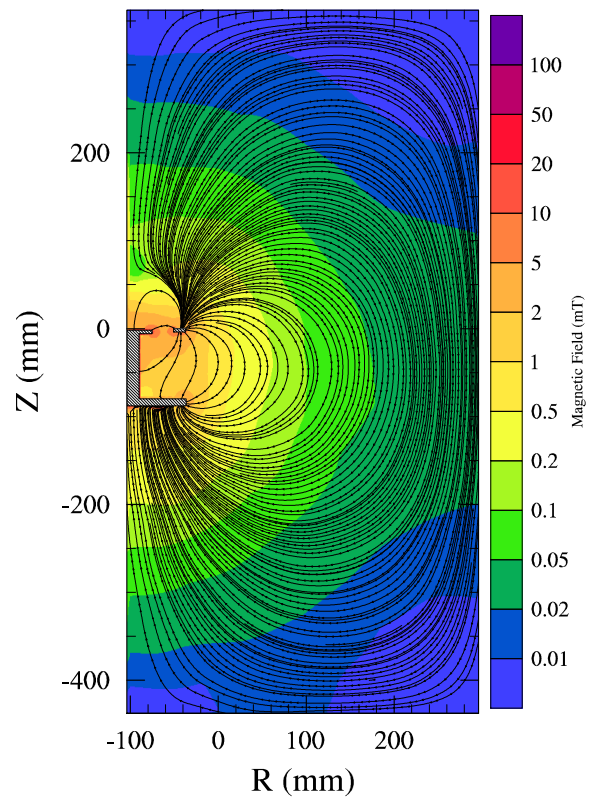
(a) $I_{\text{mag}} = 4.2 \text{ A}$



(b) $I_{\text{mag}} = 2.5 \text{ A}$



(c) $I_{\text{mag}} = 2.1 \text{ A}$



(d) $I_{\text{mag}} = 0.6 \text{ A}$

Figure 7: Modeled magnetic field magnitude and field lines.

from the cathode to the discharge chamber of the HET. Recall that the maximum voltage through which the HET ions may be accelerated is $V_{acc} = V + V_{cg}$ (where V_{cg} is negative). The thrust is given by

$$\mathbf{T} = \dot{m}\langle\mathbf{v}\rangle. \quad (3)$$

Invoking a loss term a , which incorporates cosine losses, ions which are created below the peak of the potential hill, and all other acceleration inefficiencies, the averaged exit velocity of the ions and the neutrals may be expressed as

$$\langle v \rangle = a \sqrt{\frac{2\bar{q}e(V + V_{cg})}{m_i}}. \quad (4)$$

Here \bar{q} is the average charge of all xenon species, ions and neutrals, i.e.

$$\bar{q} \equiv \frac{\sum_{q=0}^{54} qn_q}{\sum_{q=0}^{54} n_q}. \quad (5)$$

Substituting Equations 3 and 4 into Equation 2 yields

$$\eta = \frac{a^2\bar{q}em(V + V_{cg})}{m_iIV} \quad (6)$$

$$= a^2 \left(\frac{\bar{q}em}{m_iI} \right) (1 + V_{cg}/V). \quad (7)$$

$1 + V_{cg}/V$ is clearly an efficiency term, as is a^2 . The first group of terms in parentheses is the current efficiency, as defined by Ross and King.¹² Defining

$$\eta_{other} \equiv a^2 \left(\frac{\bar{q}em}{m_iI} \right) \quad (8)$$

$$\eta_{cg} \equiv 1 + V_{cg}/V \quad (9)$$

we see that the total efficiency of the thruster is given by

$$\eta = \eta_{other}\eta_{cg}. \quad (10)$$

Therefore, the maximum improvement in thruster efficiency possible by raising the cathode coupling voltage is given by

$$\eta_{max} - \eta = \eta_{other}(100\% - \eta_{cg}) \quad (11)$$

if η_{other} is independent of V_{cg} .

B. Observed Cathode Coupling Voltages

Because the cathode coupling voltage plays a significant role in determining the efficiency of the thruster, a careful look at how its behavior changes with the parameters studied is warranted. In all of the test cases presented above the cathode coupling voltage is seen to vary with cathode placement. Figure 8 shows the cathode coupling voltages for each of the anode voltages explored at optimized magnet current. One notes a general decrease in coupling voltage with increasing anode voltage. This is better seen in Figure 9. While the trend is clear, it is unclear whether the change in coupling voltage should be attributed to the change in voltage or the change in magnetic field. A most interesting feature also appears between the 200 and 150 V cases, where a drastic change in behavior is seen. We suspect that this change in behavior is not due to the change in anode voltage, but rather to the change in magnet current, and therefore magnetic field, required to operate the thruster stably at low voltage. Note that the optimal magnet current of 0.6 A for $V = 150$ V is significantly less than the optimal current of 2.1 A for $V = 200$ V. While this does not significantly change the shape of the field, it changes the magnitude (see Figure 7) which will affect how strongly the electrons are guided by the field lines.

In an attempt to better understand the effect of magnetic field strength decoupled from anode voltage, Figure 10 shows the coupling voltage for select cathode displacements as a function of magnet current. For the same anode voltage, increasing magnetic field strength generally corresponds to decreasing (more negative) coupling voltage, though

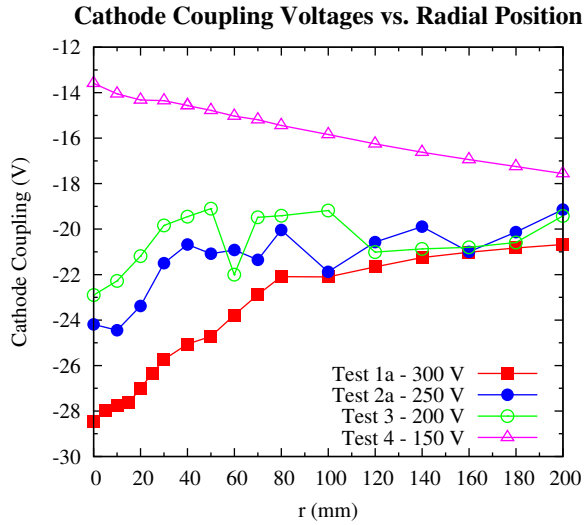


Figure 8: Cathode coupling voltages for all radial sweep tests at optimal magnet currents. The number in the legend indicates the anode voltage.

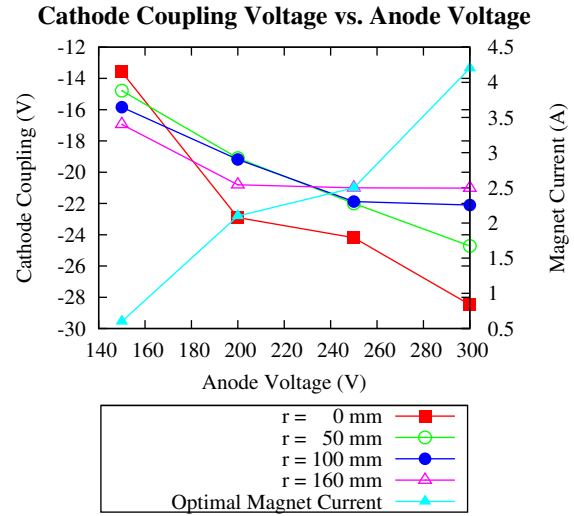


Figure 9: Cathode coupling voltages at optimal magnet current for select radial positions as a function of anode voltage.

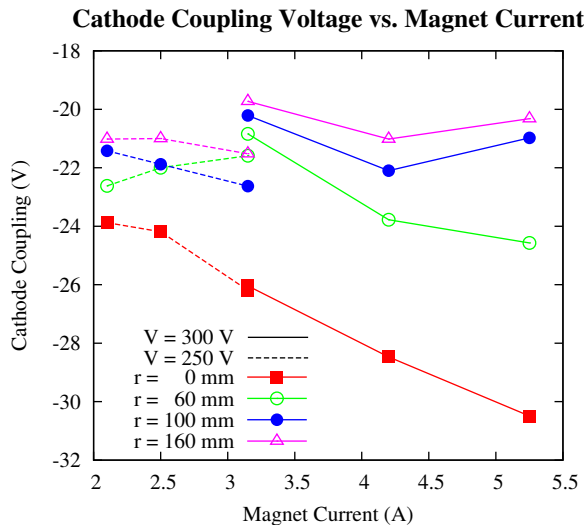


Figure 10: Cathode coupling voltages versus magnet current for the two operating voltages at which sub- and super-optimal magnet currents were set.

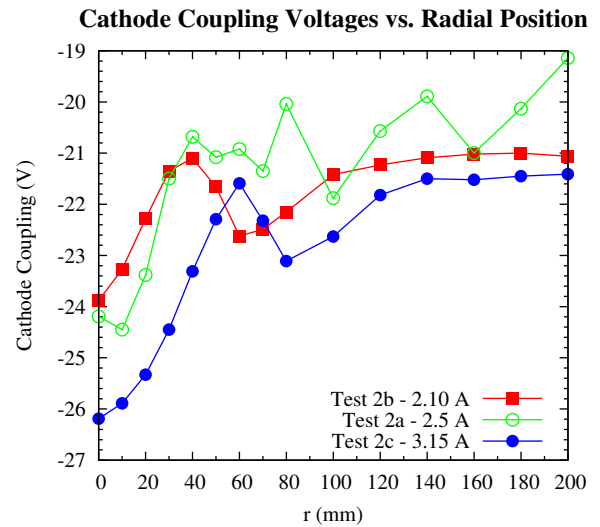


Figure 11: Cathode coupling voltages for Test 2. Note the peak near 50 mm.

this effect weakens as the cathode is moved further away from the thruster. Ross and King have also observed this behavior while operating between 100 V and 200 V on the same thruster with fixed cathode position.¹² Phenomenologically, this is reasonable as the electrons need to cross magnetic field lines in order to enter the discharge region, and electron mobility is generally inversely proportional to magnetic field strength.

One final point of interest discovered in these data is the relatively consistent local maxima of cathode coupling found in all of the Test 2 sub-cases. All of the magnet current settings in Figure 11 show a peak somewhere between 40 mm and 60 mm followed by a trough near 80 mm. This suggests that there is a narrow optimal cathode placement for a given anode voltage, at least in some circumstances. More data are needed to understand this effect.

C. Observed Thruster Efficiency

As seen in Figures 4 and 5, thruster efficiencies in this experiment are between 20% and 65%. Typical cathode coupling voltages seen in this experiment are approximately 10% of the discharge voltage, resulting in $\eta_{cg} \approx 90\%$. Solving Equation 10 for η_{other} , this suggests the other efficiencies combined are between 22% and 72%. Substituting these values into Equation 11 we conclude that raising the cathode coupling voltage to ground will result in a maximum 2.2% to 7.0% increase in efficiency, again, assuming that η_{other} is independent of V_{cg} .

Inspection of Figures 4 and 5 suggests that the changes in efficiency with cathode position are not fully accounted for by changes in cathode coupling voltage. For instance, Test 1b, in Figure 4(b), shows a 7% increase in efficiency for only a 3% change in cathode coupling voltage with respect to the discharge voltage. The 3% change in cathode coupling voltage only accounts for about 1.7% of the total 7% improvement. This suggests that either η_{other} is not independent of V_{cg} , that cathode position affects both V_{cg} and η_{other} independently, or both.

We tested the effect of grounding the cathode with the thruster running at 300 V and a mass flow of 4.0 mg/s. At each of four radial cathode locations we ran monitored the performance of the thruster with the cathode both grounded and floating. The results are plotted in Figure 12(a). The numbers printed between the traces on the graph enumerate the percentage point change in efficiency. As predicted, the data show a small increase in performance when the thruster is run with the cathode grounded. As shown in Figure 12(b), the magnitude of the change is actually less than predicted by the preceding theory, and also trends in an opposite direction. This suggests that η_{other} is not independent of V_{cg} .

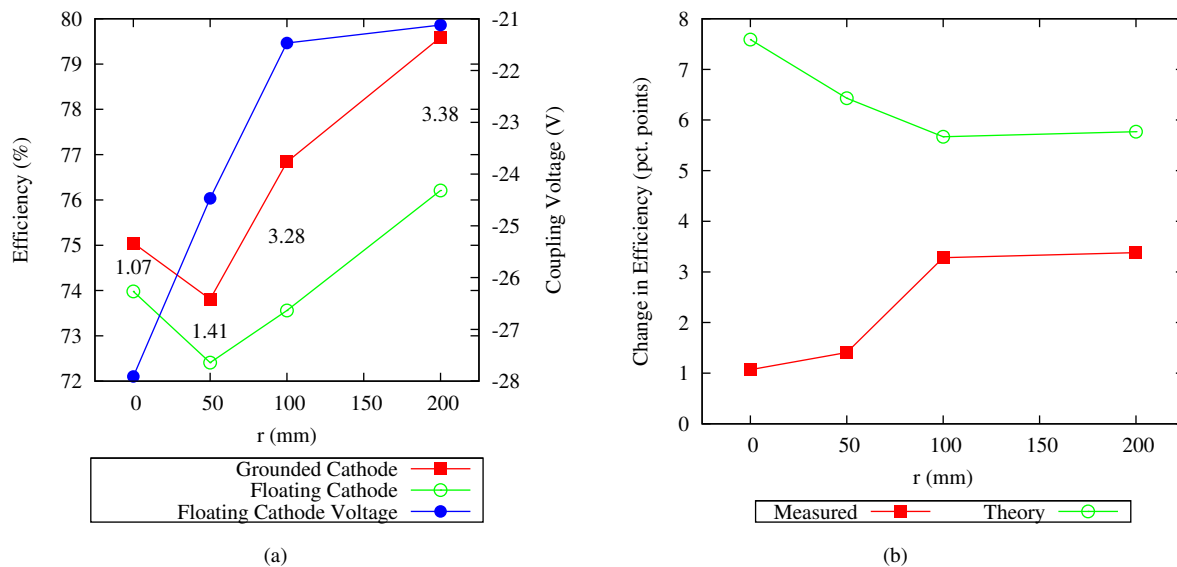


Figure 12: Comparison of thruster performance with cathode grounded and floating. (a) shows the efficiencies for four separate cathode locations for both grounded and floating operation. The numbers between the two traces are the deltas between the data. The floating cathode voltage is provided for reference. (b) shows the measured change in efficiency between grounded and floating operation along with the theoretical change according to the discussion.

The axial position sweeps in Tests 5–8 provide the clearest evidence for the connection between thruster performance, cathode coupling voltage, and cathode position. It is unclear why the axial sweep provided a larger change

than the radial sweeps. Obviously, the cathode was placed in a region where the electrons are more easily conducted to the anode. Possible explanations are that this is due to changes in magnetic field, due to the obvious change in plasma conditions (having moved into the plume), or some combination of the two. In the next section we begin the investigation of the magnetic field.

D. Performance vs. B Field

The structure of the magnetic field leads us to conclude that for the cathode to couple electrons to the HET anode, significant cross-field mobility must be occurring. There are at least three possible mechanisms. The first is classical mobility. Preliminary estimates done by the authors suggest that this is unlikely. The remaining two possibilities are plasma-fluctuation-enhanced mobility and near-wall conductivity at the face of the thruster.

Comparing the performance data from Section III with the magnetic field data proves interesting. Figure 13 overlays the field lines generated by the model on the performance results from Tests 6–8. Note that these data have only 3 radial positions, and the contours represent a considerable amount of interpolation. Regardless, one sees that the performance data tends to follow the magnetic field lines. As the cathode moves into regions of magnetic field where the electrons are directed more towards the face and more towards the channel the performance improves. The remaining data in Figures 4 and 5 support this interpretation.

This comparison suggests that performance improves when the cathode is placed such that emitted electrons are near lines which carry them closer to the discharge channel. However, since electrons are required to cross field lines no matter where there are emitted, it is not clear why the changes in performance are occurring. It is possible that when the cathode is placed in improved positions, the electrons are carried into a region of high plasma oscillations which enhances their cross-field mobility. Because the “best” field lines bring the electrons near the discharge channel where oscillations are known to occur,¹³ this seems a likely possibility. In order to test this theory, knowledge of electron temperature, plasma potential, and plasma oscillations in the likely region is necessary.

We also note that while all field lines terminate on the face, the “best” field lines terminate closer to the discharge channel. This suggests that electrons may be carried all the way to the face and from there some “near-face” conductive process injects them into the anode. The authors have begun experiments to explore this possibility, but, so far, the results have been inconclusive.

VI. Conclusions and Future Work

The means by which the cathode electrons are conducted to the discharge chamber, and their affect on cathode coupling voltage are not well understood. A better understanding of this behavior would give thruster system designers a set of tools for optimizing thruster performance without resorting to time consuming and expensive testing. The data presented here are necessary to test developing HET-cathode coupling theory.

The performance data clearly show that cathode coupling voltage and thruster performance are affected by radial and axial position and by magnetic field strength. Furthermore, the changes in cathode coupling voltage are insufficient to completely explain the changes in thruster performance through the effect of cathode coupling on acceleration potential. Therefore, either cathode position directly effects thruster efficiency, or cathode coupling voltage effects thruster behavior in a more complicated fashion than has been presented here.

We are planning future tests that will further explore the performance of the thruster with axial position. This will provide additional data against which to test cathode coupling theories. Additionally, we plan to use electrostatic probes to gather the necessary data to explore the oscillation-enhanced mobility theory, and we will continue experiments which attempt to modify the near-face conductivity.

Acknowledgments

The authors give their thanks to Mr. Jerry Ross of Michigan Tech and Dr. Bill Larson of the Air Force Research Laboratory for their discussions of thruster efficiency, to Aerojet for the donation of the BPT-2000 used in this research, and to Mr. Marty Toth for the fabrication of the cathode. Aaron Wendzel of Michigan Tech provided great help in fabricating changes to the thrust stand. This research is funded by the Air Force Office of Scientific Research and the National Science Foundation.

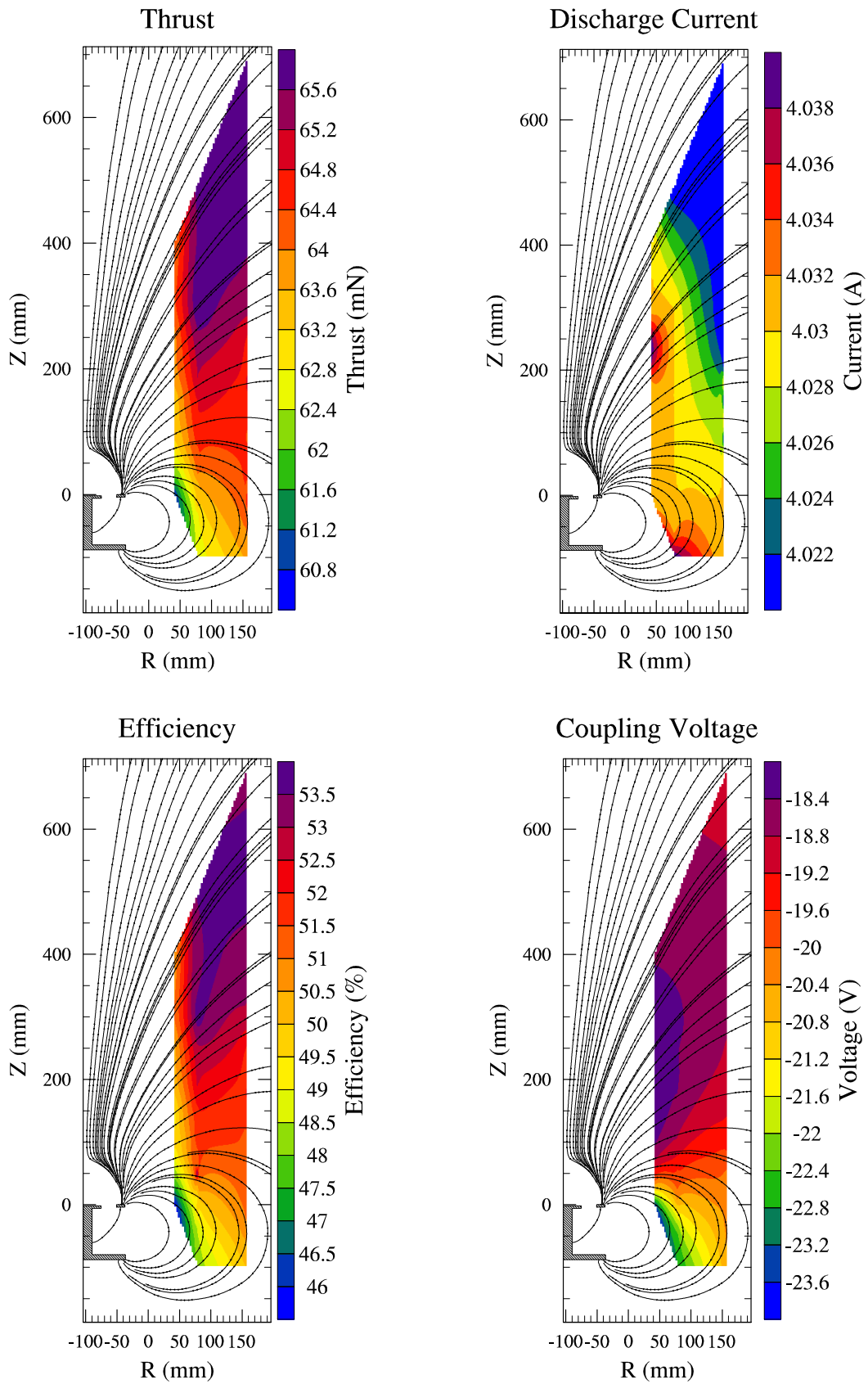


Figure 13: Performance data overlaid with magnetic field lines.

References

- ¹R. G. Jahn, *Physics of Electric Propulsion*. McGraw-Hill Series in Missile and Space Technology, New York: McGraw-Hill Book Company, 1968.
- ²L. Albarède, V. Lago, P. Lasgorceix, M. Dudeck, A. Burgova, and K. Malik, "Interaction of a hollow cathode stream with a Hall thruster," in *28th International Electric Propulsion Conference*, vol. IEPC-03-333, Electric Rocket Propulsion Society, March 17–21 2003.
- ³D. L. Tilley, K. H. de Grys, and R. M. Myers, "Hall thruster-cathode coupling," in *35th AIAA/ASME/SAE/ASEE Joint Propulsion Conference*, vol. AIAA-99-2865, June 20–24 1999.
- ⁴R. R. Hofer and A. D. Gallimore, "Recent results from internal and very-near-field plasma diagnostics of a high specific impulse Hall thruster," in *28th International Electric Propulsion Conference*, vol. IEPC-2003-037, March 17–21 2003.
- ⁵R. R. Hofer, L. K. Johnson, D. M. Goebel, and D. J. Fitzgerald, "Effects of an internally-mounted cathode on hall thruster plume properties," in *42st AIAA/ASME/SAE/ASEE Joint Propulsion Conference*, vol. AIAA-2006-4482, July 9–12 2006.
- ⁶B. E. Beal, A. D. Gallimore, and W. A. Hargus, "The effects of cathode configuration on hall thruster cluster plume properties," in *41st AIAA/ASME/SAE/ASEE Joint Propulsion Conference*, vol. AIAA-2005-3678, July 10–13 2005.
- ⁷M. Patterson, S. P. Grisnik, and G. C. Soulas, "Scaling of ion thrusters to low power," in *25th International Electric Propulsion Conference*, vol. IEPC 97-098, August 24–28 1997.
- ⁸D. H. Manzella and D. Jacobson, "Investigation of low-voltage/high-thrust Hall thruster operation," in *39th AIAA/ASME/SAE/ASEE Joint Propulsion Conference*, vol. AIAA-2003-5004, July 20–23 2003.
- ⁹A. A. Smirnov, Y. Raitses, and N. J. Fisch, "Parametric investigation of miniaturized cylindrical and annular Hall thrusters," *Journal of Applied Physics*, vol. 92, pp. 5673–5679, November 2002.
- ¹⁰J. Ashkenazy, J. Shitrit, and G. Appelbaum, "Hall thruster modifications for reduced power operation," in *29th International Electric Propulsion Conference*, vol. IEPC-2005-080, October 31–November 4 2005.
- ¹¹D. King, D. L. Tilley, R. Aadland, K. Nottingham, R. Smith, C. Roberts, V. Hraby, B. Pote, and J. Monheiser, "Development of the BPT family of U.S.-designed Hall current thrusters for commercial LEO and GEO applications," in *34th AIAA/ASME/SAE/ASEE Joint Propulsion Conference*, vol. AIAA-98-3338, July 13–15 1998.
- ¹²J. L. Ross and L. B. King, "Energy efficiency in low voltage Hall thrusters," in *43rd AIAA/ASME/SAE/ASEE Joint Propulsion Conference*, vol. AIAA-2007-5179, July 8–11 2007.
- ¹³E. Y. Choueiri, "Plasma oscillations in Hall thrusters," *Physics of Plasmas*, vol. 8, pp. 1411–1426, April 2001.